KNMI-publication; 196-I



KNMI

# Rainfall Generator for the Meuse Basin

*Simulation of 6-hourly rainfall and temperature for the Ourthe catchment*

*Rafał Wójcik and T. Adri Buishand*

De Bilt, 2001

**KNMI-publication; 196-I**

De Bilt, 2001

PO Box 201, 3730 AE De Bilt
The Netherlands
Wilhelminalaan 10
http://www.knmi.nl
Telephone +31 30 22 06 911
Telefax +31 30 22 10 407

Authors: Rafal Wójcik and T. Adri Buishand

*Work performed under contracts RI-2726 and RI-3414 to Ministry of Transport, Public works and Water Management, Institute for Inland Water Management and Waste Water Treatment RIZA, PO Box 17, 8200 AA Lelystad (The Netherlands), telephone +31 32 029 84 11, telefax +31 32 024 92 18.*

UDC: 551.524.2
551.577.2
551.579.1
556.162
(435)
(282.244.11)

ISBN: 90-369-2198-8

# Rainfall Generator for the Meuse Basin

## Simulation of 6-hourly rainfall and temperature for the Ourthe catchment

Rafał Wójcik

T. Adri Buishand

KNMI publication 196-I

Work performed under contracts RI-2726 and RI-3414 to Ministry of Transport, Public Works and Water Management, Institute for Inland Water Management and Waste Water Treatment RIZA, P.O. Box 17, 8200 AA Lelystad (The Netherlands) Telephone: +31.320.298411; Telefax: +31.320.249218

# CONTENTS

# SUMMARY

This report presents a first study on the development of a stochastic weather generator for the Meuse basin which produces long-duration , multi-site time series of precipitation and temperature. By running these synthetic data through a hydrological/hydraulic model, it is expected to get a better insight into the likelihood of extreme river discharges in the Netherlands. This report is restricted to the Ourthe basin (3626 $km^2$). Time series of 6-hourly area-average precipitation of 3 sub-catchments (Ourthe upstream of Hamoir, Amblève and Vesdre) and average 6-hourly temperature at St. Hubert are considered.

Simulation is done by nearest-neighbour resampling. Because of the intended application, the performance of the method is only assessed for the winter half-year (October-March). It appears that straightforward resampling of the historical 6-hourly values does not adequately reproduce a number of second-order statistics of precipitation and temperature. Particularly, the slow decay of the autocorrelation function of 6-h area-average rainfall is not preserved. The standard deviations of monthly rainfall and the quantiles of the multi-day winter maximum precipitation amounts are therefore underestimated. As an alternative, simulation of daily values with disaggregation into 6-h values using the method of fragments is studied. With this strategy a reasonable reproduction of the second-order statistics of rainfall and temperature is achieved. Moreover, there is a good correspondence between the historical and simulated distributions of the winter maximum precipitation amounts.

# 1. Introduction

## 1.1. Background

The Rhine and the Meuse are the most important rivers in the Netherlands. A large part of the country is situated in their delta. Protection against flooding is a point of continuous concern. Dikes and other flood protection works in the non-tidal part of the rivers have to withstand a discharge that is exceeded once in 1250 years (Middelkoop and van Haselen, 1999). Traditionally this design discharge has been obtained from a statistical analysis of peak discharges (data from 1901 for the Rhine and from 1911 for the Meuse). An extensive evaluation of the design discharge for the Rhine was done by the first Boertien Commission (Delft Hydraulics and EAC-RAND, 1993). The design discharge for the Meuse received much less attention. However, shortly after the commission had completed its work a large Meuse flood occurred in the south of the Netherlands. The second Boertien Commission was then appointed to formulate prevention measures to reduce future impacts of floods. For this commission a much more detailed analysis of the extreme Meuse discharges was performed than under its predecessor (Delft Hydraulics, 1994).

The determination of the 1250-year discharge event from statistical information in a record of about 100 years involves a strong extrapolation, which is quite uncertain. The extrapolation does not take into account the physical properties of the river basin. Therefore the first Boertien Commission suggested developing a hydrological/hydraulic model for the river basin of interest. The Institute for Inland Water Management and Waste Water Treatment (RIZA) adopted this idea in a research plan for a new methodology to determine the design discharge (Bennekom and Parmet, 1998). Besides the hydrological/hydraulic model, the development of a stochastic rainfall generator was also planned in order to produce long-duration rainfall series, containing unprecedented extreme events. This new methodology does not only provide the peak discharges but also the temporal patterns of these extreme events and thus may give a better insight into the profile of the design discharge. Moreover, the new methodology also offers prospects to assess the potential impacts of climate change.

After a pilot study (Buishand and Brandsma, 1996), KNMI started in 1996 with the development of a stochastic rainfall generator for the Rhine basin. A nearest-neighbour resampling technique was used to generate multi-site daily precipitation and temperature series (Wójcik et al., 2000). The resampling technique is basically the same as that in Young (1994) and Rajagopalan and Lall (1999) for generating multivariate time series of daily weather variables at a single site.

This report presents a first study to develop a stochastic rainfall generator for the Meuse basin. The Meuse originates on the plateau of Langres in northeastern France

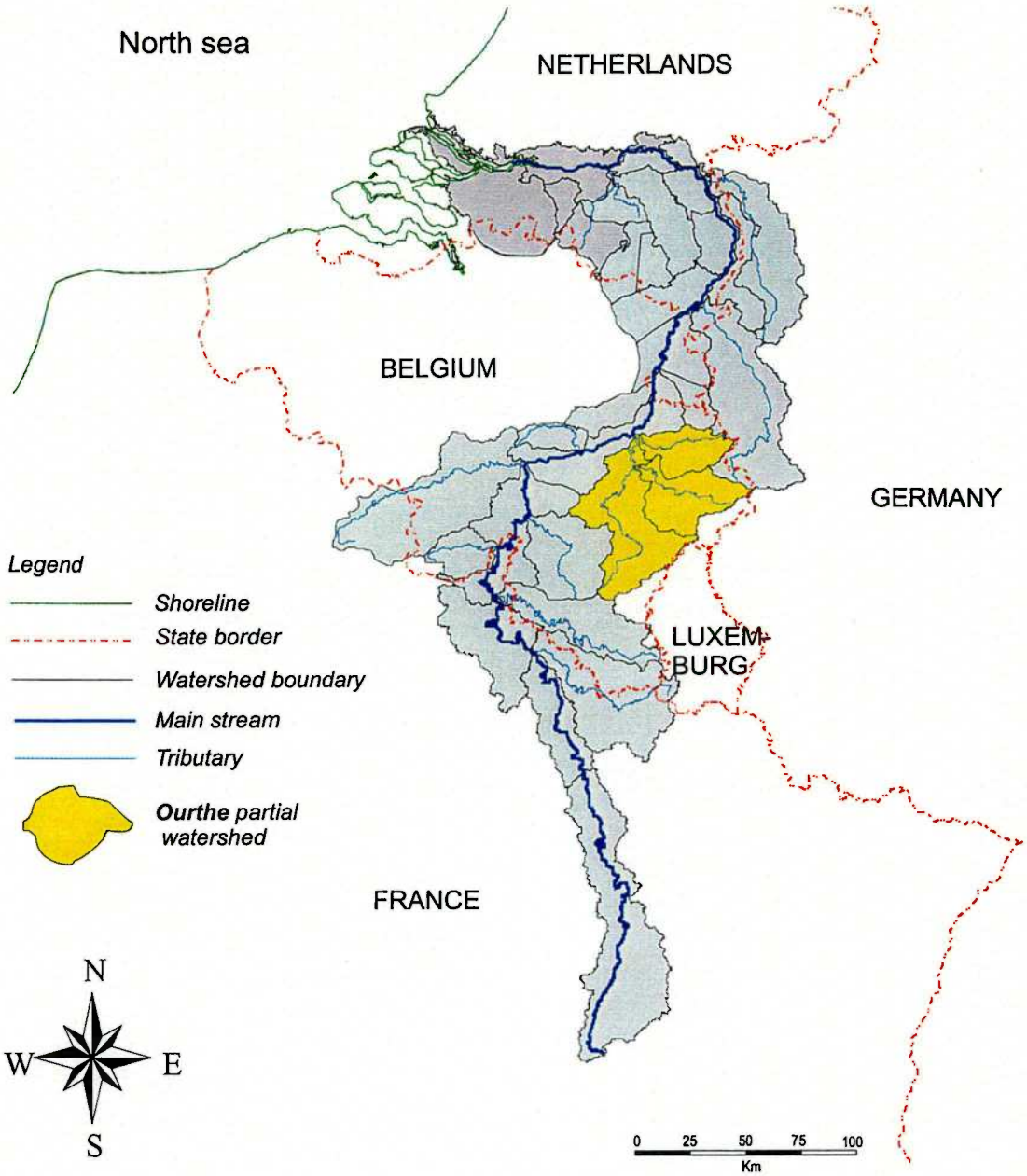


Figure 1.1: The Meuse basin

(Fig. 1.1) at an altitude of 409 m. After passing through France and the Belgian Ardennes, it enters the Netherlands a few kilometres to the south of Maastricht. The catchment area upstream of this town is about 22 000 km$^2$ whereof about 12 000 km$^2$ in Belgium. Due to a number of steep tributaries, the river discharge at Maastricht quickly reacts on the rainfall over the Belgian Ardennes if the catchment is wet. It was therefore decided to generate 6-hourly values for the Meuse basin instead of daily values. Because of the 6-hourly time step, developing a rainfall generator for the Meuse basin is not a trivial duplication of the work for the Rhine basin. The temporal correlation of 6-hourly

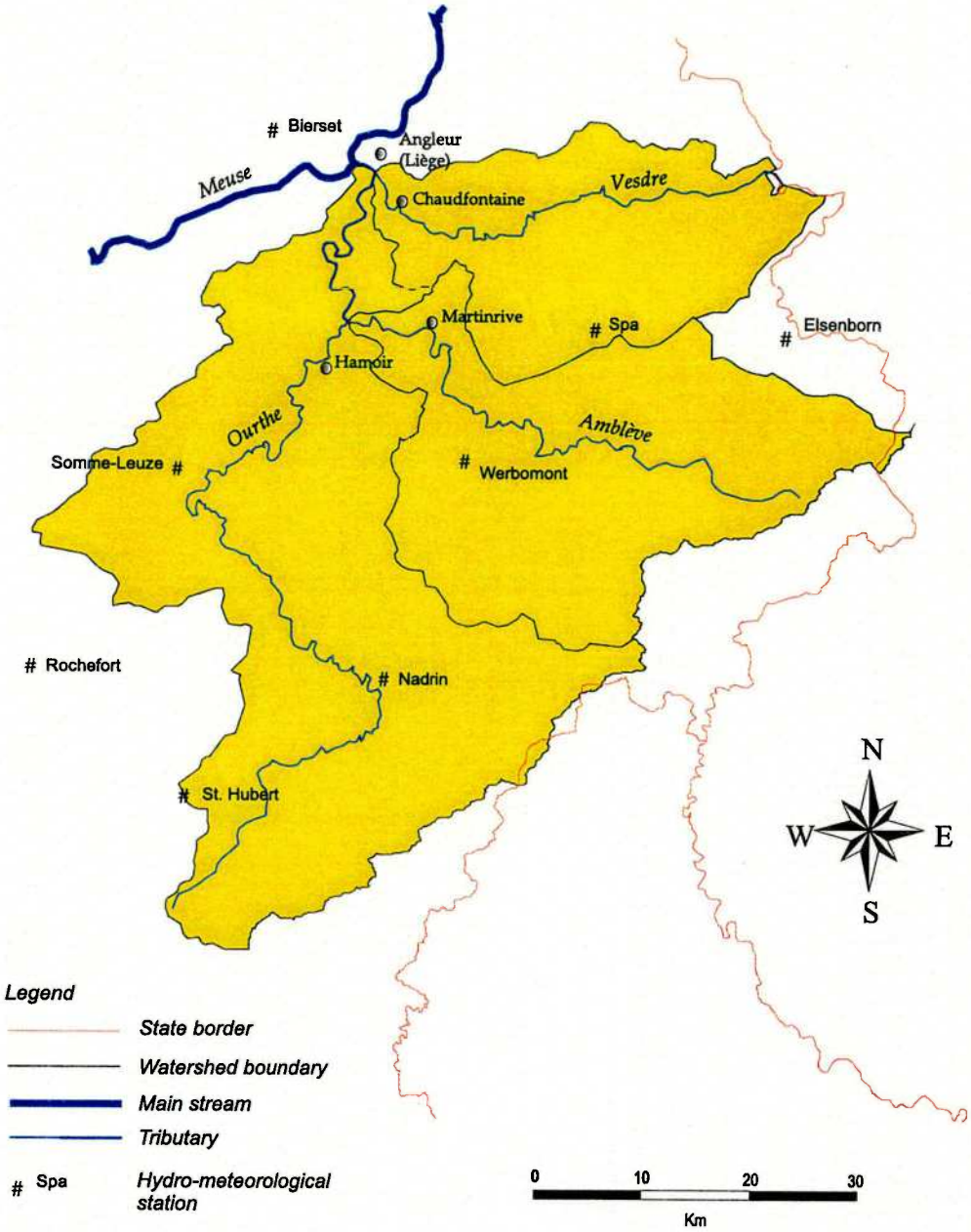


Figure 1.2: The Ourthe partial watershed

rainfall is different from that of daily rainfall. Moreover, 6-hourly rainfall can only be obtained for a limited number of stations and these records are often incomplete. In this first work with sub-daily data only the Ourthe basin (Fig. 1.1) is considered. With an area of 3626 km$^2$ it is the largest sub-basin of the Meuse. Two important tributaries are the Amblève and the Vesdre (Fig. 1.2). The altitude ranges between 60 m at the Meuse confluence to nearly 700 m in the eastern part of the basin.

## 1.2. Overview of the report

This report is organized as follows. Section 2 describes the data used in this study and some technical issues related to preprocessing of these data. Section 3 outlines two strategies for the simulation of 6-hourly values of rainfall and temperature. The statistical techniques used are discussed in Section 4. Section 5 presents the results of simulations performed with the two resampling strategies. To evaluate the quality of those simulations, second-order statistics of rainfall and temperature and Gumbel plots of maximum rainfall for different durations are analyzed. The two final sections address conclusions from the research and recommendations for the practical application.

# 2. Data description

## 2.1. Basic material

Simulation of 6-hourly rainfall and temperature values by nearest-neighbour resampling requires historical data with the same temporal resolution. For the Ourthe basin 1-hourly precipitation data from 8 hydrometeorological stations in, or close to, the basin (see Fig.1.2) and daily catchment-average precipitation data for the entire basin and 3 sub-catchments of the basin (Ourthe upstream of Hamoir, Amblève and Vesdre) were available. These two data sources were combined to produce 6-hourly area-average precipitation of the sub-catchments. For temperature there were 3-hourly records from 3 stations in the basin. Data for the 32-year period 1967-1998 were used. These data were provided by the Royal Meteorological Institute of Belgium (RMIB).

## 2.2. 6-hourly station precipitation and temperature data

Station data with the required 6-hourly resolution were obtained by aggregating 1-hourly precipitation values and averaging 3-hourly temperatures, respectively. To perform this simple operation, it must be kept in mind that daily rainfall at ordinary climatological stations in Belgium has always been recorded at 8 national time (this corresponds to 0700 GMT in winter and 0600 GMT in summer). Therefore, for the winter season 6-hourly rainfall amounts were calculated for the intervals 7-13, 13-19, 19-1 and 1-7 GMT. The corresponding 6-hourly temperatures were then taken as averages of the 3-hourly temperature pairs falling within the corresponding rainfall measurement intervals (9,12; 15,18; 21,0; 3,6 GMT). In summer, the recording times for precipitation shift one hour backwards.

It turned out that a lot of values in the analysed 6-hourly records were missing. Sometimes instead of the standard "99999" code, 0's were inserted during a period of instrument failure. In both cases, the data were not used to produce 6-hourly catchment average rainfall (see Section 4.2.1). Table 2.1 shows the proportion of missing values in the precipitation and temperature data as identified with the standard code. For most stations in the Ourthe basin this proportion ranges from 1-10%. There are, however two stations, Elsenborn and Somme-Leuze, with much more missing data. This is due to the fact that sub-daily precipitation measurements in those stations started after 1967 (1987 in Elsenborn and 1973 in Somme-Leuze). The station Spa was not operational during 1987-1989. For temperature the most complete data set is that for St. Hubert. Because the Ourthe basin covers a relatively small area and spatial dependence of the temperature is large, it is sufficient to consider the temperature at St. Hubert only. Missing values in this record were supplemented by the temperature at Nadrin plus a

Table 2.1: Percentage of missing values in 6-hourly rainfall and temperature time series for several stations in or around the Ourthe basin for the period 1967-1998. In the lower part of the table the total number of records in each of the analysed series is listed.

| Nr | Station | Missing values [%] | |
|---|---|---|---|
| | | Precipitation | Temperature |
| 1 | Bierset | 2.1 | not available |
| 2 | Spa | 9.8 | not available |
| 3 | Elsenborn | 64.0 | not available |
| 4 | Werbomont[1] | 4.7 | not available |
| 5 | Somme-Leuze | 29.9 | not available |
| 6 | Nadrin [2] | 5.9 | 2.8 |
| 7 | Rochefort | 6.5 | 1.4 |
| 8 | St. Hubert | 0.4 | 0.2 |
| Number of records | | 46748 | 46748 |

[1] Concatenation of measurements at Werbomont and Chêne-al-Pierre
[2] Concatenation of measurements at Odeigne, Tailles and Nadrin

correction of -0.5 °C to account for systematic differences between the two stations. From a comparison between the average maximum an minimum temperatures at Nadrin and St. Hubert in Sneyers and Vandiepenbeeck (1981) it appeared that there is no diurnal or seasonal cycle in the differences between the two stations.

## 2.3. Daily area-average precipitation data

The RMIB routinely calculates daily area-average precipitation for a number of catchments in Belgium. These averages are obtained from station data with the Thiessen method. In that method one assumes that the rainfall at any point in the catchment is the same as that at the nearest rainfall station. The area-average $\overline{P}$ can be written as:

$$\overline{P} = \sum_{j=1}^{N} \lambda_j P_j \tag{2.1}$$

where $P_j$ is the amount of rainfall of the $j$th station ($j = 1, ..., N$). To calculate the Thiessen weights $\lambda_j$ the catchment is covered with a rectangular grid and for each grid point lying within the catchment the closest rainfall station is searched. The proportion of grid points assigned to a rainfall station gives the weight $\lambda_j$ for that station.

Table 2.2: Sub-catchmets of the Ourthe that have been used in this study.

| | Name of the catchment | Size [km$^2$] |
|---|---|---|
| Total area | Ourthe at Angleur | 3626 |
| Sub-area 1 | Ourthe at Hamoir | 1597 |
| Sub-area 2 | Amblève at Martinrive | 1044 |
| Sub-area 3 | Vesdre at Chaudfontaine | 677 |
| Remaining area | – | 308 |

Table 2.3: Largest negative rainfall amount [mm] in the remaining area of the Ourthe basin in the period of 1967-1998 .

| Date | sub-area 1 | sub-area 2 | sub-area 3 | total area | remaining area |
|---|---|---|---|---|---|
| 19940714 | 8.5 | 7.4 | 2.6 | 5.9 | -5.4 |

Table 2.2 shows that the three sub-catchments do not fully cover the entire Ourthe basin. The daily rainfall for the remaining area was estimated as :

$$[3626 \times P(\text{Total area}) - 1597 \times P(\text{Sub-area 1}) - 1044 \times P(\text{Sub-area 2}) - 677 \times P(\text{Sub-area 3})]/308$$

This, however, frequently results in a negative value. The largest negative amount occurs on 14 July 1994 as listed in Table 2.3. The annual average of the negative values is no more than -17 mm (see Table 2.4). This kind of inconsistency in the data is mainly caused by :

- the use of different grid lengths for different sub-catchments in the derivation of Thiessen weights
- the use of different scales and grid origins for different sub-catchments (this influences the decision to which grid points a given measurement station will be associated and whether a particular grid point near the catchment boundary is within the basin or not, what in turn, affects the area-average precipitation)

For application with the hydrological/hydraulic model, it is recommended to replace the negative daily rainfall amounts for the remaining area by zeros.

Table 2.4: Annual average rainfall for the whole basin and sub-catchmets of the Ourthe that have been used in this study (the means are for the period 1967-1998) .

| | Name of the catchment | Mean annual precipitation [mm] |
|---|---|---|
| Total area | Ourthe at Angleur | 1092 |
| Sub-area 1 | Ourthe at Hamoir | 968 |
| Sub-area 2 | Amblève at Martinrive | 1092 |
| Sub-area 3 | Vesdre at Chaudfontaine | 1096 |
| Remaining area (positive amounts) | – | 918 |
| Remaining area (negative amounts) | – | -17 |

# 3. STRATEGIES

As a result of different types of the historical precipitation data in the Ourthe basin there are different strategies for generating 6-h values by resampling. Two different approaches are outlined in this section.

**Method 1: Simulation of 6-h area-average rainfall and station temperature**

In this approach the daily area-average rainfall data of 3 sub-catchments of the Ourthe basin are disaggregated into 6-hourly values first. The available 6-hourly station rainfall series form the basis for the disaggregation (for details see section 4.2.1). After this preprocessing procedure, the resampling of 6-hourly catchment-average rainfall and 6-hourly station temperature is performed. The key steps in this method are:

**Step 1** Disaggregate the daily area-average rainfall into 6-hourly area-average rainfall.

**Step 2** Generate 6-hourly area-average rainfall over sub-catchments and 6-hourly station temperature for St. Hubert.

**Method 2: Simulation of daily values with disaggregation into 6-hourly values**

A starting point in this method is simulation of historical records of daily catchment-average rainfall and average daily temperature for St. Hubert. The resampled values are then disaggregated using the method of fragments (for details see Section 4.2.2). For the disaggregation the 6-hourly catchment-average rainfall from step 1 of the previous method and 6-hourly station temperatures are used. The key steps in this algorithm are:

**Step 1** Simulate daily precipitation and temperature data using historical records.

**Step 2** Disaggregate the daily area-average rainfall and daily station temperature into 6-hourly area-average rainfall and 6-hourly station temperature, respectively.

In both methods, the rainfall for the remaining area of the Ourthe basin can be passively simulated as it was done with precipitation and temperature for high-elevation stations in Switzerland in the resampling procedure for the Rhine basin (Wójcik et al., 2000).

# 4. Methods

## 4.1. Nearest-neighbour resampling

In the nearest-neighbour method weather variables like precipitation and temperature are sampled simultaneously with replacement from the historical data. Temporal dependence is incorporated by conditioning on preceding values. For instance, to generate weather variables for a new day $t + 1$, one first abstracts the days from the historical record with similar characteristics as those simulated for the previous day. One of these nearest

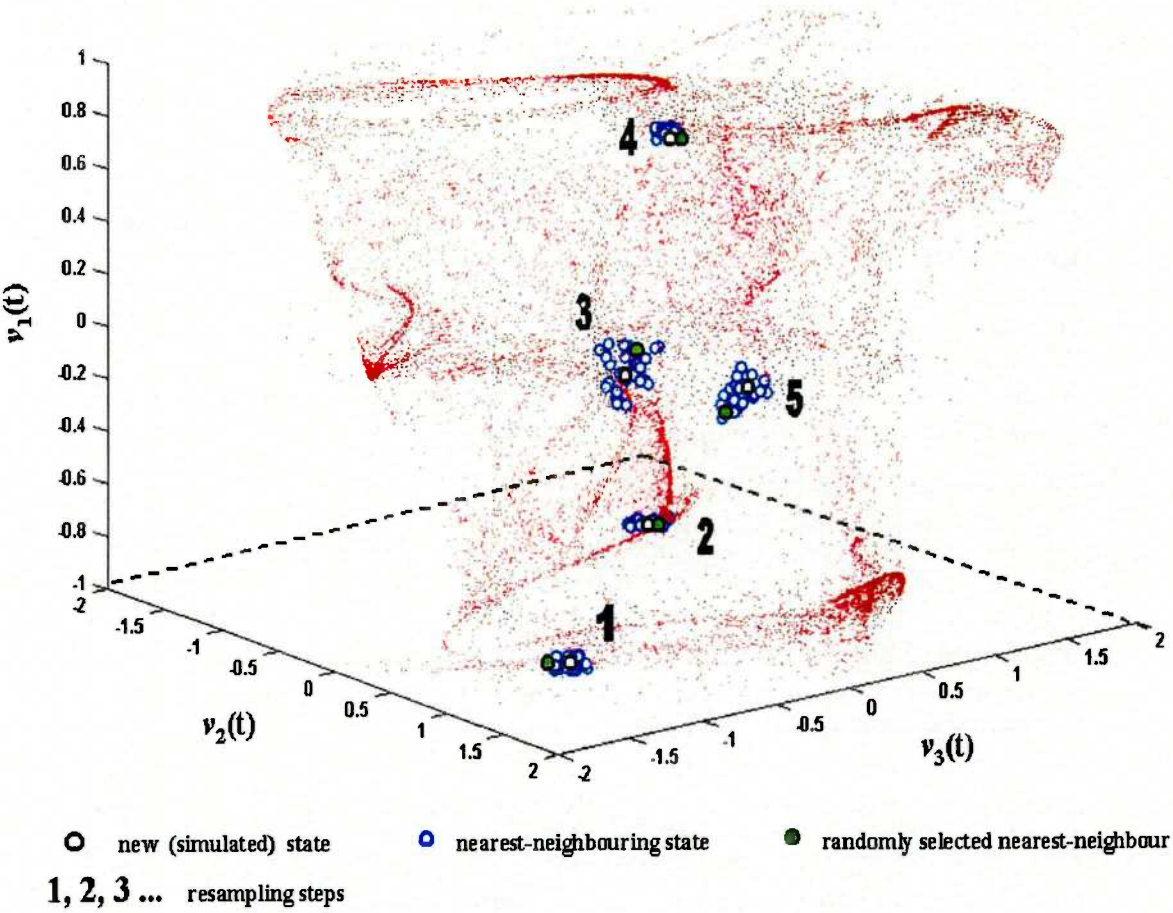


Figure 4.1: The principle of nearest-neighbour resampling

neighbours is randomly selected and the observed values for the day subsequent to that nearest neighbour are adopted as the simulated values for day $t+1$. A feature (or state) vector $\mathbf{D}_t$ is used to find the nearest neighbours in the historical record.

Figure 4.1 shows an example of the first five steps of nearest-neighbour resampling in a 3-D state space (so $\mathbf{D}_t = [v_1(t), v_2(t), v_3(t)]^T$ ). The points in the state space (red dots) were obtained by iterating a parametric set of 3 non-linear, state equations described by Pickover (1990). The three state variables in this illustration do not have any particular physical meaning. One could, however, consider them as three relevant weather variables, like e.g., temperature, precipitation and air pressure. To initialize the simulation, one of the historical states is selected at random. This state is depicted in Fig. 4.1 as a white dot with label 1. Next, the collection of $k = 30$ states (blue dots) which lie closest to the white dot is determined. One of those nearest neighbours (green dot) is then selected at random and its successor (a white dot with label 2) is adopted as the simulated state for $t = 2$. Thereafter, again a set of $k$ nearest neighbours is determined, one of them is randomly selected and its successor (white dot with label 3) is delivered as the simulated state for $t = 3$. The above procedure is repeated a large number of times.

An important issue in nearest-neighbour resampling is the choice of a function which measures distance between points in the state space. By using this function (also called metric) one identifies the $k$ nearest neighbours of a particular state. In this study the *Mahalanobis metric* (for broader discussion see Wójcik et al., 2000) is used. For two $q$-dimensional state vectors $\mathbf{D}_t$ and $\mathbf{D}_u$ the latter is defined as:

$$\delta_{\mathrm{Mh}}(\mathbf{D}_t, \mathbf{D}_u) = \left((\mathbf{D}_t - \mathbf{D}_u)^T \mathbf{B}^{-1} (\mathbf{D}_t - \mathbf{D}_u)\right)^{\frac{1}{2}} \tag{4.1}$$

where $\mathbf{B}$ is the covariance matrix of the feature vector $\mathbf{D}_t$. The elements of this matrix are the covariances between the components of $\mathbf{D}_t$:

$$B_{ij} = \mathrm{Cov}(v_i(t), v_j(t)) \ , \quad i, j = 1, ..., q \tag{4.2}$$

When the feature vector components are assumed to be uncorrelated, $\mathbf{B}$ becomes the variance matrix with elements:

$$B_{ij} = \begin{cases} \mathrm{Var}(v_i(t)) & \text{if } i = j, \\ 0 & \text{otherwise} \end{cases} \tag{4.3}$$

A discrete probability distribution or kernel is required for resampling from the $k$ nearest neighbours. Lall and Sharma (1996) recommended a kernel that gives higher weight to the closer neighbours. For this decreasing kernel the probability $p_n$ that the $n$th closest neighbour is resampled is given by:

$$p_n = \frac{1/n}{\sum_{i=1}^{k} 1/i}, \quad n = 1, ..., k \tag{4.4}$$

From the above description it is clear that apart from creating a feature vector, choosing a metric and a probability kernel, the user has to set the number $k$ of nearest neighbours. In this study we use $k = 5$ which seems to work well in practice as shown in Brandsma and Buishand (1999).

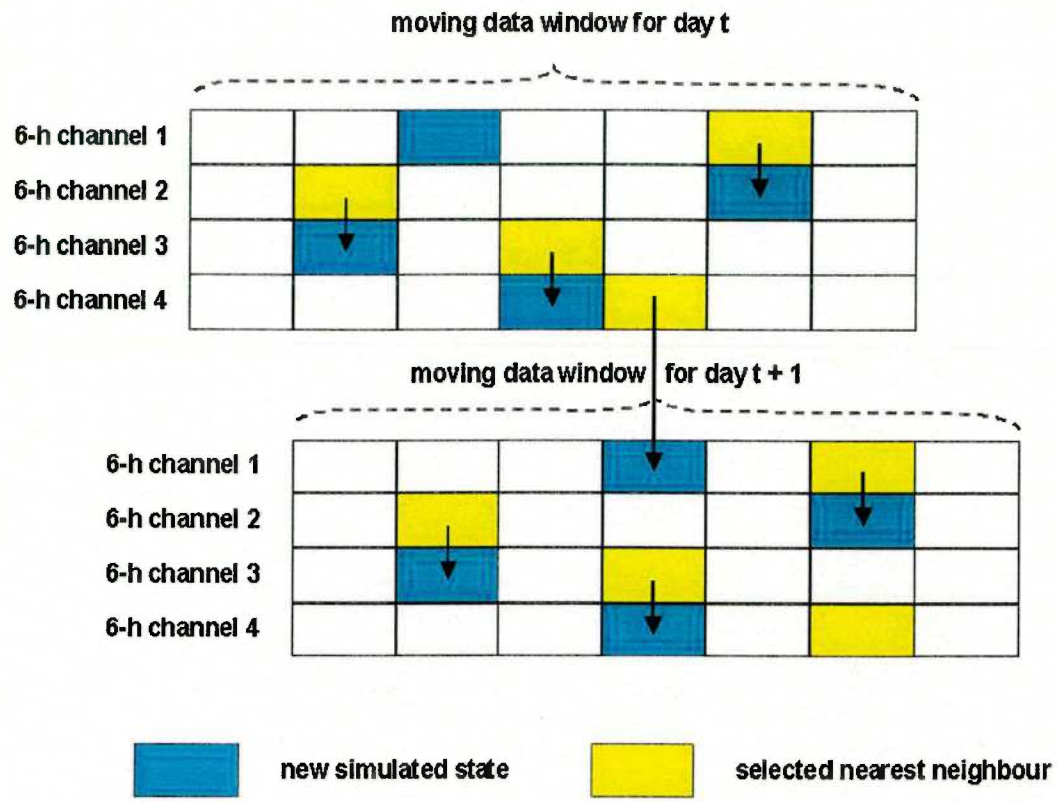


Figure 4.2: The concept of channels in 6-hourly nearest-neighbour resampling

To reduce the effect of seasonal variation, the search for nearest neighbours is restricted to days within a moving window, centered on the calendar day of interest. For rainfall and temperature simulations the width of this window ($W_{\mathrm{mw}}$) was 61 days as in Brandsma and Buishand (1999). Yet another technical issue arises when straightforward simulation of 6-hourly values (Method 1) is performed. The search for nearest neighbours is then further restricted to preserve the diurnal variation. The 6-h values are divided into four channels. The first channel contains the data from the first 6-hourly interval, the second channel contains the data from the second 6-hourly interval, etc. Figure 4.2 shows the use of channels in nearest-neighbour resampling of 6-hourly values. In the beginning of the simulation the moving data window is centered on day $t = 1$ (in this case $W_{\mathrm{mw}}$=7 days). Then, an initial state is selected at random (blue rectangle) from 6-h channel 1. Within this channel a nearest neighbour of the initial state (yellow rectangle) is randomly selected and its successor (blue rectangle in 6-h channel 2) is adopted as a simulated state for the next 6-h time step. One proceeds in a similar manner for the next steps. The only point of attention is when the successor of the nearest neighbour

from channel 4 has to be found. This successor is delivered from channel 1 which is this time, however, bounded by the moving window centered on the next day $t + 1$.

## 4.2. Disaggregation procedures

### 4.2.1. Observed rainfall

Historical records of daily catchment-average rainfall of 3 sub-catchments of the Ourthe and the remaining area were disaggregated into 6-hourly catchment-average rainfall using the following formula:

$$\overline{P}^{i}_{t,j} = w^{i}_{t}\,\overline{P}_{t,j}, \quad i = 1,\ldots,4; \;\; t = 1,\ldots,365J; \;\; j = 1,\ldots,4 \tag{4.5}$$

where $\overline{P}^{i}_{t,j}$ is the 6-h area-average rainfall of the $j$th area for the $i$th 6-h channel of day $t$, $\overline{P}_{t,j}$ is the daily area-average rainfall, $w^{i}_{t}$ is a disaggregation weight and $J$ is the total number of years in the historical record. The weights in (4.5) are calculated as ratios:

$$w^{i}_{t} = \frac{P^{i}_{t}}{\sum_{i=1}^{4} P^{i}_{t}} \tag{4.6}$$

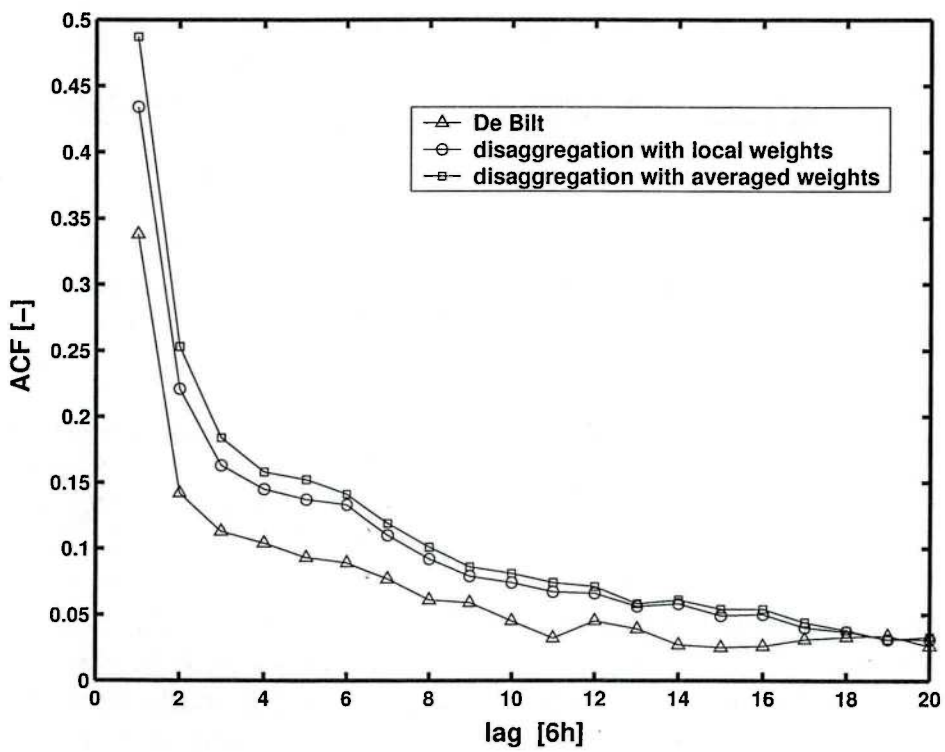


Figure 4.3: Autocorrelation function (ACF) of disaggregated 6-hourly catchment-average rainfall for the Ourthe basin and 6-hourly station rainfall from De Bilt. The autocorrelation coefficients for catchment-average rainfall are mean values taken over 3 sub-catchments.

where $P_t^i$ is the 6-hourly rainfall amount at the station situated closest to the geometrical center of the $j$th sub-catchment. In the case that there is no rainfall at this station or that there are missing values the next closest station is searched for and the disaggregation is performed using the 6-h rainfall amounts from that station. If, however, for a particular day $t$ no station rainfall is available, the weights $w_t^i$ in (4.5) were set to 0.25 (uniform disaggregation).

**A cautionary remark**
It should be noted, however, that this rough method does not reproduce the statistics of real 6-h catchment-average rainfall. One may expect that especially the variance of the disaggregated data will be too large. In consequence, these data may contain some spurious peaky rainfall events. On the other hand, such a physical artifact might be compensated by adjusting relevant parameters in the hydrological model which, after this study, will be used to transform the 6-h catchment-average rainfall into discharge.

The above method of estimating the weights locally or station-wise is not the only possible approach. Alternatively, these coefficients can be determined by taking an average of all the local weights $w_{t,l}^i$ obtained with (4.6) for all stations with non-missing rainfall data:

$$w_t^i = \frac{1}{L} \sum_{l=1}^{L} w_{t,l}^i \tag{4.7}$$

where $L$ refers to the number of stations. The two weighting schemes were compared in terms of the autocorrelation function (ACF) of the disaggregated 6-h rainfall. Figure 4.3 shows that both approaches give similar values of the autocorrelation coefficients. Unfortunately, it is difficult to verify these results, since there are no measured 6-h catchment averages. Anyway, the autocorrelation in disaggregated 6-hourly catchment-average rainfall is stronger than that in 6-h station rainfall (see Fig. 4.3) as it should be for area-average rainfall.

### 4.2.2. Simulated rainfall and temperature

For disaggregation of simulated daily catchment-average rainfall and temperature the method of fragments by Maheepala and Perera (1996) was adapted. The term fragments refers to the weights $w_t^i$ in (4.5). The method is a special case of nearest-neighbour resampling. In order to preserve the dependence between the 6-hourly values at the transition of two days, the selection of a nearest neighbour for the disaggregation of the simulated daily rainfall and temperature data for a particular day $t$ considers both these daily data and the data of the last 6-h channel of the previous day $t-1$. For a mathematical description of the selection process the following vector pairs are defined:

$$\begin{aligned} \mathbf{X}_t &= [x_1(t), x_2(t), \ldots, x_n(t)]^T \\ \widehat{\mathbf{X}}_u &= [\widehat{x}_1(u), \widehat{x}_2(u), \ldots, \widehat{x}_n(u)]^T \end{aligned} \tag{4.8}$$

and

$$\begin{aligned} \mathbf{\Phi}_{t-1} &= [\phi_1(t-1), \phi_2(t-1), \ldots, \phi_n(t-1)]^T \\ \widehat{\mathbf{\Phi}}_{u-1} &= [\widehat{\phi}_1(u-1), \widehat{\phi}_2(u-1), \ldots, \widehat{\phi}_n(u-1)]^T \end{aligned} \tag{4.9}$$

where $x_i(t)$ is the simulated daily value of the $i$th weather variable ($i = 1, \ldots, n$) for day $t$, $\widehat{x}_i(u)$ is the daily value obtained by summing (for rainfall) or averaging (for temperature) 6-hourly historical values of the $i$th weather variable for day $u$, $\phi_i(t-1)$ is the value of the $i$th weather variable simulated in the last 6-h channel for day $t-1$ and $\phi_i(u-1)$ is the historical value of the $i$th weather variable in the last 6-h channel for day $u-1$. The symbol $n$ refers to the total number of simulated weather variables. In this study $n = 4$ since there are 3 area-average rainfall variables and 1 temperature variable. For each simulated day $t$, the distances:

$$\alpha_u = ((\mathbf{X}_t - \widehat{\mathbf{X}}_u)^T \mathbf{C}^{-1} (\mathbf{X}_t - \widehat{\mathbf{X}}_u))^{\frac{1}{2}} \tag{4.10}$$

$$\beta_u = ((\mathbf{\Phi}_{t-1} - \widehat{\mathbf{\Phi}}_{u-1})^T \mathbf{G}^{-1} (\mathbf{\Phi}_{t-1} - \widehat{\mathbf{\Phi}}_{u-1}))^{\frac{1}{2}} \tag{4.11}$$

are calculated for all days in the historical record falling within a moving window of width $W_{\text{mw}} = 61$. The matrices $\mathbf{C}$ and $\mathbf{G}$ are the covariance matrices of $\mathbf{X}_t$ and $\mathbf{\Phi}_{t-1}$ respectively, defined analogous to (4.2) or (4.3). Then the day $u^\star$ is found such that:

$$u^\star = \min_u (\alpha_u + \beta_u) \tag{4.12}$$

The 6-h values of the relevant weather variables for day $u^\star$ are then used to disaggregate the simulated daily values of those variables for day $t$. For precipitation the disaggregation is performed by applying (4.5) and (4.6), which preserve the daily precipitation totals. In order to preserve the daily mean temperature the following additive structure is used:

$$T_t^i = T_{u^\star}^i + \overline{T}_t - \overline{T}_{u^\star} \tag{4.13}$$

where $T_t^i$ is the disaggregated temperature for the $i$th channel of day $t$, $T_{u^\star}^i$ is the historical temperature for the $i$th channel of the selected day $u^\star$, $\overline{T}_t$ is the simulated average temperature for day $t$ and

$$\overline{T}_{u^\star} = \frac{1}{4} \sum_{i=1}^{4} T_{u^\star}^i \tag{4.14}$$

## 4.3. Standardization

Before resampling the data were deseasonalized through standardization. The daily temperature was standardized by subtracting an estimate $m_d$ of the mean and dividing by an estimate $s_d$ of the standard deviation for the calendar day $d$ of interest:

$$\widetilde{x}_t = (x_t - m_d)/s_d, \quad t = 1, ..., 365J; \quad d = (t-1) \bmod 365 + 1 \tag{4.15}$$

where $x_t$ and $\widetilde{x}_t$ are the original and standardized variables for day $t$, respectively, and $J$ is the total number of years in the record. The estimates $m_d$ and $s_d$ were obtained

by smoothing the sample mean and standard deviation of the successive calendar days using the Nadaraya-Watson smoother (for technical details see Wójcik et al., 2000, p.16). Daily precipitation was standardized by dividing by a smooth estimate $m_{d,\text{wet}}$ of the mean wet-day precipitation amount:

$$\widetilde{x_t} = x_t / m_{d,\text{wet}}, \quad t = 1, ..., 365J; \quad d = (t-1) \bmod 365 + 1 \tag{4.16}$$

A wet day was defined here as a day with $P \geq 0.1$ mm. For 6-hourly temperature and precipitation data (4.15) and (4.16) were applied to each 6-hourly channel separately.

## 4.4. Model identification

Simulations of precipitation and temperature values were performed with two different temporal resolutions: 6-hourly resolution (Method 1) and daily resolution (first step of Method 2). In both cases the unconditional resampling model was applied. This implies that the state vector $\mathbf{D}_t$ comprises generated variables for the previous 6h or the previous day, depending on the time resolution considered. To keep the dimension of the state vector small the arithmetic mean of the standardized area-average precipitation of 3 sub-catchments was used as its first element and the standardized temperature for St. Hubert as the second one. Additionally, for 6-hourly simulations the inclusion of generated variables for the two previous 6-hourly time steps was studied. This resampling scheme is designated as second-order model. The Mahalanobis distance was incorporated in all simulation models. For 6-h simulations, the covariance matrix $\mathbf{B}$ defined by (4.2) or (4.3) was calculated in two ways:

- globally for the entire set of standardized weather variables, yielding the global covariance (GC) or global variance (GV) model respectively
- locally, i.e. using only the values of the standardized weather variables lying within the moving data window and within a particular channel, yielding the local covariance (LC) or local variance (LV) model respectively

Daily values of precipitation and temperature were generated with the LC model only. To disaggregate these values (second step of Method 2), the nearest-neighbour search was conducted using (4.10) and (4.11) where the matrices $\mathbf{C}$ and $\mathbf{G}$ were computed according to the GC, GV, LC and LV schemes.

# 5. Results

## 5.1. Reproduction of standard deviations and autocorrelation

Extreme river discharges in the Meuse basin are mostly caused by prolonged heavy rainfall in winter. The reproduction of the standard deviations of 6-hourly station temperature and area-average precipitation, the standard deviations of the monthly average temperature and the monthly precipitation totals, and the 6-hourly autocorrelation coefficients is therefore only presented for the winter half-year (October - March). To reduce the influence of the annual cycle these statistics were first calculated for each calendar month separately. For each of the analyzed weather variables the winter estimates were obtained by taking the arithmetic mean over the six winter months (October, ..., March). The effect of the diurnal cycle was accounted for by using separate values for the mean of each channel in the calculation of autocorrelation coefficients.

Ten runs of 32 years were generated to investigate the performance of the resampling procedures (Method 1 and Method 2). For rainfall of each sub-catchment and temperature at St. Hubert, the standard deviations and autocorrelation coefficients were first estimated for each simulation run separately and then averaged over the 10 runs. The average estimates $\overline{s_{6h}}^*$, $\overline{s_M}^*$, $\overline{r}^*(l)$ of the standard deviations of the 6-hourly and monthly values and the lag $l$ autocorrelation coefficient respectively, were compared with the estimates $\overline{s_{6h}}$, $\overline{s_M}$, $\overline{r}(l)$ for the historical data. The relative difference $\Delta\overline{s_{6h}}$ between the observed and simulated 6-hourly standard deviation is calculated using:

$$\Delta\overline{s_{6h}} = (\overline{s_{6h}}^* - \overline{s_{6h}})/\overline{s_{6h}} \quad 100\% \tag{5.1}$$

with a similar equation for the average relative difference $\langle\Delta\overline{s_M}\rangle$ of the monthly standard deviation, and

$$\Delta\overline{r}(l) = [\overline{r}^*(l) - \overline{r}(l)], \quad l = 1, ..., 5 \tag{5.2}$$

for the difference $\Delta\overline{r}(l)$ of the lag $l$ autocorrelation coefficient. For rainfall, the above mentioned differences were further averaged over 3 sub-catchments. In order to evaluate the statistical significance of $\Delta\overline{s_{6h}}$, $\Delta\overline{s_M}$ and $\Delta\overline{r}(l)$ standard errors *se* were calculated for the estimates from the historical record. The standard errors were obtained with the jackknife method in Buishand and Beersma (1996). A criterion of $2 \times se$ was used to indicate significant differences between the historical and simulated values. This roughly corresponds to a two-sided test at the 5% level (Brandsma and Buishand, 1998). Tables 5.1 and 5.2 present $\Delta\overline{s_{6h}}$, $\Delta\overline{s_M}$ and $\Delta\overline{r}(l)$ for the 6-hourly simulations pertaining to Method 1 and the second step of Method 2 respectively. Note that for precipitation, instead of presenting $\Delta\overline{r}(3)$, $\Delta\overline{r}(4)$, $\Delta\overline{r}(5)$ separately, the average difference $\overline{\Delta\overline{r}(3,4,5)}$ taken over these three lags is shown. For the first-order 6-h resampling models (GV1,

GC1, LV1, LC1), Table 5.1 shows that a number of statistics are not well reproduced. A surprisingly large and statistically significant bias is present in the standard deviations of monthly rainfall. This behaviour is caused by a strong underestimation of the higher order autocorrelation coefficients ($l > 2$). The first-order models are simply not able to deal with the slow decay of the autocorrelation function in the 6-h rainfall data. This also applies to the second-order models (GV2, GC2, LV2, LC2). Moreover, the simulations with those models suffer from a significant underestimation of the mean.

Table 5.2 displays more optimistic results for Method 2. Despite the rather large bias in the first two autocorrelation coefficients of disaggregated rainfall, the differences at higher lags are much smaller than those in Method 1. In consequence, the quality of reproduction of $\overline{s_M}$ is much better than in the straightforward 6-h simulations. For the same reason the negative bias in the standard deviations of monthly temperatures is much smaller than in Method 1. Furthermore, Table 5.2 shows that the way the covariance matrices are computed has some impact on the performance of the disaggregation procedure. Both for rainfall and temperature, the differences $\Delta\overline{r}(1)$ and $\Delta\overline{r}(2)$ are smallest for the LV model.

Table 5.1: Performance of the direct simulation of 6-hourly values (Method 1; ten runs of 32 years in each case) for the winter (October-March). For each statistic the differences (mean precipitation in mm, mean temperature in °C and autocorrelation coefficients dimensionless) or percentage differences (standard deviations) are given between the simulated and historical data (1967-1998). The historical values of the mean and standard deviations in the bottom line are in mm (precipitation) or °C (temperature). Estimates in bold differ more than $2 \times se$ from the estimates for the historical data.

| | mean | | $\Delta\overline{s_M}$ | | $\Delta\overline{s_{6h}}$ | | $\Delta\overline{r}(1)$ | | $\Delta\overline{r}(2)$ | | $\overline{\Delta\overline{r}(3,4,5)}$ |
|---|---|---|---|---|---|---|---|---|---|---|---|
| Case | $P$ | $T$ | $P$ | $T$ | $P$ | $T$ | $P$ | $T$ | $P$ | $T$ | $P$ |
| GV1 | -2.6 | **0.1** | **-25.2** | **-10.3** | -0.7 | -2.3 | -0.007 | **-0.008** | 0.001 | -0.005 | **-0.061** |
| GC1 | -2.4 | **0.1** | **-25.9** | **-12.7** | -1.1 | -3.1 | -0.009 | **-0.009** | 0.005 | -0.006 | **-0.052** |
| LV1 | -3.3 | 0.0 | **-23.9** | **-12.3** | -0.9 | -2.5 | -0.007 | **-0.009** | -0.005 | -0.006 | **-0.057** |
| LC1 | -3.2 | 0.0 | **-26.1** | -9.2 | -1.6 | -1.4 | -0.014 | -0.006 | -0.004 | 0.000 | **-0.057** |
| GV2 | **-7.3** | **0.3** | **-27.1** | **-15.8** | -4.0 | -5.2 | -0.005 | **-0.025** | -0.004 | **-0.034** | **-0.047** |
| GC2 | **-12.6** | **0.3** | **-32.1** | **-24.2** | **-6.6** | **-4.8** | -0.019 | **-0.034** | -0.010 | **-0.063** | **-0.060** |
| LV2 | **-10.3** | **0.3** | **-28.8** | **-14.3** | **-6.1** | **-5.0** | -0.022 | **-0.026** | 0.003 | **-0.037** | **-0.045** |
| LC2 | **-14.3** | **0.3** | **-32.9** | **-26.1** | **-7.7** | **-5.1** | -0.002 | **-0.036** | -0.009 | **-0.070** | **-0.058** |
| Historical | 91.3 | 2.6 | 47.5 | 1.9 | 1.8 | 4.1 | 0.435 | 0.930 | 0.221 | 0.846 | 0.148 |

Table 5.2: Performance of the simulation of daily values followed by disaggregation into 6-hourly values (Method 2; ten runs of 32 years in each case) for the winter (October-March). For each statistic the differences (mean precipitation in mm, mean temperature in °C and autocorrelation coefficients dimensionless) or percentage differences (standard deviations) are given between the simulated and historical data (1967-1998). The historical values of the mean and standard deviations in the bottom line are in mm (precipitation) or °C (temperature). Estimates in bold differ more than $2 \times se$ from the estimates for the historical data.

| | mean | | $\Delta\overline{s_M}$ | | $\Delta\overline{s_{6h}}$ | | $\Delta\overline{r}(1)$ | | $\Delta\overline{r}(2)$ | | $\overline{\Delta\overline{r}(3,4,5)}$ |
|---|---|---|---|---|---|---|---|---|---|---|---|
| Case | $P$ | $T$ | $P$ | $T$ | $P$ | $T$ | $P$ | $T$ | $P$ | $T$ | $P$ |
| GV | -2.4 | **0.1** | -6.8 | -3.3 | 1.5 | -0.01 | **-0.043** | -0.017 | **-0.041** | **-0.021** | -0.019 |
| GC | -2.4 | **0.1** | -6.8 | -3.3 | 0.7 | -0.03 | **-0.035** | -0.016 | **-0.027** | **-0.019** | -0.014 |
| LV | -2.4 | **0.1** | -6.8 | -3.3 | -0.3 | -0.09 | **-0.022** | -0.012 | -0.018 | **-0.017** | -0.014 |
| LC | -2.4 | **0.1** | -6.8 | -3.3 | 0.7 | -0.03 | **-0.036** | -0.015 | **-0.029** | **-0.018** | -0.014 |
| Historical | 91.3 | 2.6 | 47.5 | 1.9 | 1.8 | 4.1 | 0.435 | 0.930 | 0.221 | 0.846 | 0.148 |

## 5.2. Winter maximum precipitation amounts

A number of 320-year simulations were performed with Method 1 and Method 2. For three of these simulations (GC1, GV2 and LV) Figure 5.1 shows Gumbel plots of the 6-h, 1,4 and 10-day winter precipitation maxima averaged over the 3 sub-catchments. In the

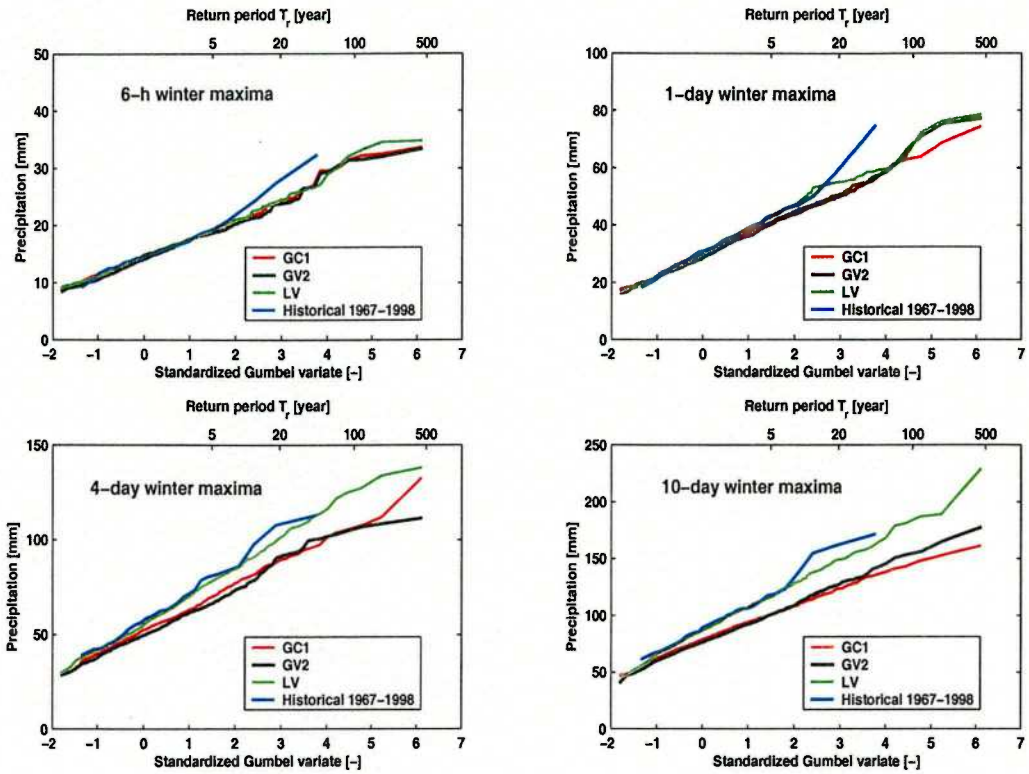


Figure 5.1: Gumbel plots of 6-h, 1,4 and 10-day winter precipitation maxima for historical and simulated data (runs of 320 years)

case of 6-h and 1-day maxima there is a reasonable correspondence between the historical and simulated distributions. Moreover, for both durations the simulated Gumbel curves show a tendency towards flattening at the level of maximum historical precipitation. The maxima in the simulated data are slightly above the highest historical value. In Method 1, slight exceedances of the highest 6-hourly precipitation amount are possible due to:

- the use of a smoothed seasonally varying mean to standardize the historical data before resampling (see Section 4.3)
- the use of the moving window, which allows for resampling of rainfall values outside the boundaries of the winter half-year

For the same reasons the highest 1-day winter maxima generated in Step 1 of Method 2 may exceed the highest 1-day precipitation amounts in the historical record. Disaggregation of the daily precipitation amounts by the method of fragments may also result in exceedances of the highest historical 6-h precipitation amount. For 4-day and 10-day

precipitation, only the LV model from Method 2 is able to reproduce the distribution of the historical data properly. In the other two simulations (GC1 and GV2) displayed in Fig. 5.1, the Gumbel curves lie below the curve for the historical data. This striking underestimation of the extreme precipitation amounts is due to the poor reproduction of the autocorrelation function (especially at higher lags) and the underestimation of the mean and standard deviation by those two models.

To further explore the behaviour of model LV one extra run of 1000-years was performed. The Gumbel plots for this simulation are depicted in Fig. 5.2. It is again clear

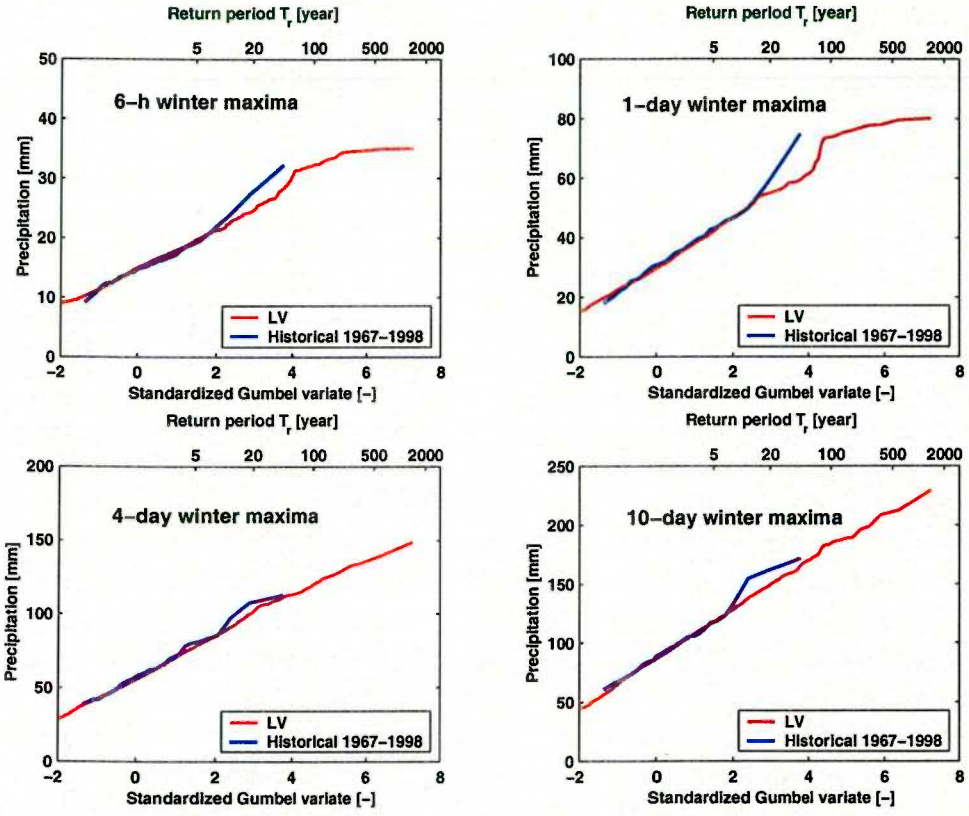


Figure 5.2: Gumbel plots of 6-h, 1,4 and 10-day winter precipitation maxima for historical and simulated data (LV model, one run of 1000 years)

that the generated 6-h and 1-day extreme precipitation events are a little bit higher than those in the historical record. For the longer durations (4 and 10-day) the curves for the simulated maxima are almost perfect straight lines which implies that their distribution is in good agreement with the Gumbel distribution.

# 6. Conclusions

The purpose of this study was to perform simulations of 6-hourly rainfall and temperature for the Ourthe basin. The time series of 6-hourly area-average precipitation of 3 sub-catchments of the Ourthe and average 6-hourly temperature from 1 station in the basin were used. The 6-hourly area-average precipitation amounts were obtained from the daily average using a rough disaggregation procedure. Two different methods were compared: straightforward simulation of 6-hourly values (Method 1) and simulation of daily values with disaggregation into 6-hourly values (Method 2). In both cases unconditional nearest-neighbour resampling was used as a simulation routine. In Method 2 disaggregation was performed with the method of fragments.

The simulations in Method 1 were not able to reproduce a number of second-order statistics of observed rainfall and temperature properly. Particularly the standard deviations of monthly rainfall were significantly underestimated. This negative bias was mainly due to the inability to reproduce the slow decay of the autocorrelation function of 6-h rainfall. Introduction of second-order models to tackle this problem remained without success. Because of the above deficiency the quantiles of the simulated 4 and 10-day maximum precipitation amounts were lower than those in the historical record.

More optimistic results were obtained with Method 2. Both for rainfall and temperature the second-order statistics were reproduced much better than in Method 1. Moreover, the distributions of the simulated rainfall maxima were quite close to those from the historical record. A single simulation run of 1000 years demonstrated that for longer durations (4 and 10-day) the generated maxima remain in good agreement with the Gumbel distribution, also outside the range of the historical data.

Summarizing, it is clear that this study revealed a serious flaw of nearest-neighbour resampling as a method to straightforwardly generate area-average rainfall and station temperature with a temporal resolution of 6 hours. This technique, however, performs well on the daily time scale so it is possible to combine it with a disaggregation procedure to obtain the required finer scale (6-hourly) values as demonstrated with Method 2.

# 7. RECOMMENDATIONS

The value of the simulation method should be carefully tested. It is strongly recommended to calibrate the hydrological model with the same rainfall and temperature series used in this report, i.e., area-average rainfall for the three sub-catchments and the station temperature for St. Hubert. Evapotranspiration requires particular attention. Area-average potential evapotranspiration is available for sub-catchments, but is not directly simulated. The need for a more advanced disaggregation procedure to obtain 6-hourly average catchment rainfall should be considered.

Because the statistical properties of historical precipitation and temperature were best preserved by resampling model LV in Method 2, this model should be investigated further. In particular the study of the synthetic discharges at the basin outlet in Angleur resulting from the use of simulated precipitation and temperature data would be of interest. The gain of using a 6-hourly time step instead of a daily time step should be explored. If there is no gain only the generation of daily values should be developed further for the Meuse basin.

To discriminate deficiencies in the resampling model from those in hydraulic and hydrological modelling, the validation procedure should comprise a comparison of extreme value characteristics of the observed discharges over the period 1967-1998 with those of the

- corresponding 6-h discharges computed from the historical (disaggregated) 6-hourly catchment-average rainfall and 6-hourly station temperature at St. Hubert over the period 1967-1998, and
- corresponding 6-h discharges computed from the simulated 6-hourly catchment-average rainfall and 6-hourly station temperature at St. Hubert.

Several 32-year simulations should be considered to obtain accurate estimates of the extreme-value characteristics for the resampling model used and to get some idea of the uncertainty of these estimates.

# Acknowledgements

We thank W. van de Langemheen and W.E. van Vuuren (RIZA) for useful discussions. The constructive comments of J.J. Beersma (KNMI) on computer programs developed in this study are gratefully acknowledged. The precipitation and temperature data from Belgium were made available by the Royal Meteorological Institute of Belgium (RMIB). G.R. Demarée and Ms. S. Derasse (RMIB) are kindly acknowledged for clarifying some problems with the daily catchment-average precipitation data. The maps of the Meuse and Ourthe basins were made by W.E. van Vuuren.

# REFERENCES


Bennekom, A. R. V. and Parmet, B. W. A. H. (1998). *Bemessungsabfluß in den Niederlanden; menschliche Einflüsse und andere Unsicherheiten*, pages 125–131. In: Zukunft der Hydrologie in Deutschland, BfG Mitteilung 16. Bundesanstalt für Gewässerkunde, Koblenz.

Brandsma, T. and Buishand, T. A. (1998). Simulation of extreme precipitation in the Rhine basin by nearest-neighbour resampling. *Hydrol. Earth Syst. Sci.*, 2:195–209.

Brandsma, T. and Buishand, T. A. (1999). Rainfall generator for the Rhine basin: Multi-site generation of weather variables by nearest-neighbour resampling. KNMI-publication 186-II, KNMI, De Bilt.

Buishand, T. A. and Beersma, J. J. (1996). Statistical tests for comparison of daily variability in observed and simulated climates. *J. Climate*, 9:2538–2550.

Buishand, T. A. and Brandsma, T. (1996). Rainfall generator for the Rhine catchment: a feasibility study. Technical Report TR-183, KNMI, De Bilt.

Delft Hydraulics (1994). Onderzoek watersnood Maas. 15 vol., Delft, the Netherlands.

Delft Hydraulics and EAC-RAND (1993). Toetsing uitsgangpunten rivierdijkversterkingen, Deelrapport 2: Maatgevende belastingen. Delft Hydraulics, Emmeloord, and European American center for Policy Analysis (EAC-RAND), Delft, the Netherlands.

Lall, U. and Sharma, A. (1996). A nearest neighbor bootstrap for resampling hydrologic time series. *Water Resour. Res.*, 32:679–693.

Maheepala, S. and Perera, B. J. C. (1996). Monthly hydrologic data generation by disaggregation. *J. Hydrol.*, 178:277–291.

Middelkoop, H. and van Haselen, C. O. G., eds. (1999). Twice a river. Rhine and Meuse in the Netherlands. RIZA report no. 99003, RIZA, Arnhem.

Pickover, C. (1990). *Computers, Pattern, Chaos and Beauty. Graphics from an Unseen World.* St. Martin's Press, New York.

Rajagopalan, B. and Lall, U. (1999). A k-nearest-neighbor simulator for daily precipitation and other variables. *Water Resour. Res.*, 35:3089–3101.

Sneyers, R. and Vandiepenbeeck, M. (1981). Les normales du réseau thermométrique belge. IRMB publication 106-A, IRMB, Bruxelles.

Wójcik, R., Beersma, J. J., and Buishand, T. A. (2000). Rainfall generator for the Rhine basin: Multi-site generation of weather variables for the entire drainage area. KNMI-publication 186-IV, KNMI, De Bilt.

Young, K. C. (1994). A multivariate chain model for simulating climatic parameters from daily data. *J. Appl. Meteorol.*, 33:661–671.

## OVERZICHT VAN KNMI-PUBLICATIES, VERSCHENEN SEDERT 2000

### KNMI-PUBLICATIE MET NUMMER

186-II Rainfall generator for the Rhine Basin: multi-site generation of weather variables by nearest-neighbour resampling / T. Brandsma a.o.

186-III Rainfall generator for the Rhine Basin: nearest-neighbour resampling of daily circulation indices and conditional generation of weather variables / Jules J. Beersma and T. Adri Buishand

186-IV Rainfall generator for the Rhine Basin: multi-site generation of weather variables for the entire drainage area / Rafal Wójcik, Jules J. Beersma and T. Adri Buishand

188 SODA workshop on chemical data assimilation: proceedings; 9-10 December 1998, KNMI, De Bilt, The Netherlands

189 Aardbevingen in Noord-Nederland in 1998: met overzichten over de periode 1986-1998 / [Afdeling SO]

190 Seismisch netwerk Noord-Nederland / [afdeling Seismologie]

191 Het KNMI-programma HISKLIM (HIStorisch KLIMaat) / T. Brandsma, F. Koek, H. Wallbrink, G. Können

192 Gang van zaken 1940-48 rond de 20.000 zoekgeraakte scheepsjournalen / Hendrik Wallbrink en Frits Koek

193 Science requirements document for OMI-EOS / contr. by R. van der A .. [et al.] **(limited distribution)**

194-1 De zonsverduistering van 11 augustus 1999, deel 1: de waarnemingen van het gedrag van flora en fauna / J. Kuiper, m.m.v. Guus Kauffeld

195 An optimal infrasound array at Apatity (Russian Federation) / Läslo Evers and Hein Haak **(limited distribution)**

### TECHNISCH RAPPORT = TECHNICAL REPORT (TR)

219 De invloed van de grondwaterstand, wind, temperatuur en dauwpunt op de vorming van stralingsmist: een kwantitatieve benadering / Jan Terpstra

220 Back-up modellering van windmeetmasten op luchthavens / Ilja Smits

221 PV-mixing around the tropopause in an extratropical cyclone / M. Sigmond

222 NPK-TIG oefendag 16 december 1998 / G.T. Geertsema, H. van Dorp e.a.

223 Golfhoogteverwachtingen voor de Zuidelijke Noordzee: een korte vergelijking van het ECMWF-golfmodel (EPS en operationeel), de nautische gidsverwachting, Nedwam en meteoroloog / D.H.P. Vogelezang, C.J. Kok

224 HDFg library and some hdf utilities: an extention to the NCSA HDF library user's manual &reference guide / Han The

225 The Deelen Infrasound Array: on the detection and identification of infrasound / L.G. Evers and H.W. Haak

226 2D Variational Ambiguity Removal / J.C.W. de Vries and A.C.M. Stoffelen

227 Seismo-akoestische analyse van de explosies bij *S.E. Fireworks* ; Enschede 13 mei 2000 / L.G. Evers e.a.

228 Evaluation of modified soil parameterization in the ECMWF landsurface scheme / R.J.M. IJpelaar

229 Evaluation of humidity and temperature measurements of Vaisala's HMP243 plus PT100 with two reference psychrometers / E.M.J. Meijer

230 KNMI contribution to the European project WRINCLE: downscaling relationships for precipitation for several European sites / B.-R. Beckmann and T.A. Buishand

231 The Conveyor Belt in the OCCAM model: tracing water masses by a Lagrangian methodology / Trémeur Balbous and Sybren Drijfhout

232 Analysis of the Rijkoort-Weibull model / Ilja Smits

233 Vectorization of the ECBilt model / X. Wang and R.J. Haarsma

234 Evaluation of a plant physiological canopy conductance model in the ECMWF land surface scheme / J. van de Kassteele

235 Uncertainty in pyranometer and pyrheliometer measurements at KNMI in De Bilt / J.S. Henzing and W.H. Knap

236 Recalibration of gome spectra for the purpose of ozone profile retrieval / Ronald van der A

### WETENSCHAPPELIJK RAPPORT = SCIENTIFIC REPORT (WR)

00-01 A model of wind transformation over water-land surfaces / V.N. Kudryavtsev et al.

00-02 On the air-sea coupling in the WAM wave model / D.F.Doortmont and V.K. Makin.

00-03 Salmon's Hamiltonian approach to balanced flow applied to a one-layer isentropic model of the atmosphere / W.T.M. Verkley

00-04 On the behaviour of a few popular verification scores in yes-no forecasting / C.J. Kok

01-01 Hail detection using single-polarization radar / Iwan Holleman

01-02 Comparison of modeled ozone distributions with ozonesonde observations in the tropics / Rob Put

01-03 Impact assessment of a doppler wind lidar in space on atmospheric analyses and numerical weather prediction / G.J. Marseille, A. Stoffelen, F. Bouttier, C. Cardinali, S. de Haan and D. Vasiljevic.